

# Geometric Mechanics Applied to Tetrapod Locomotion on Granular Media

Yasemin Ozkan Aydin<sup>1</sup>(✉), Baxi Chong<sup>4</sup>, Chaohui Gong<sup>4</sup>, Jennifer M. Rieser<sup>1</sup>, Jeffery W. Rankin<sup>2</sup>, Krijn Michel<sup>2</sup>, Alfredo G. Nicieza<sup>3</sup>, John Hutchinson<sup>2</sup>, Howie Choset<sup>4</sup>, and Daniel I. Goldman<sup>1</sup>

<sup>1</sup> School of Physics, Georgia Institute of Technology, Atlanta, GA, USA  
{yasemin.ozkanaydin,jennifer.rieser,daniel.goldman}@physics.gatech.edu

<sup>2</sup> Royal Veterinary College, London, UK  
jwrankin@gmail.com, {kmichel,JHutchinson}@rvc.ac.uk

<sup>3</sup> Universidad Oviedo, Asturias, Spain  
agnicz@gmail.com

<sup>4</sup> Carnegie Mellon University, Pittsburgh, PA, USA  
baxichong8@gmail.com, chaohuigong@gmail.com, choset@cs.cmu.edu

**Abstract.** This study probes the underlying locomotion principles of earliest organisms that could both swim and walk. We hypothesize that properly coordinated leg and body movements could have provided a substantial benefit toward locomotion on complex media, such as early crawling on sand. In this extended abstract, we summarize some of our recent advances in integrating biology, physics and robotics to gain insight into tetrapod locomotor coordination and control principles. Here, we observe crawling salamanders as a biological model for studying tetrapod locomotion on sloped granular substrates. Further, geometric mechanics tools are used to provide a theoretical framework predicting efficacious body motions on yielding terrain. Finally, we employ these coordination strategies on a robophysical salamander model traversing a sandy slope. This analysis of salamander-like robotic motion in granular media can be seen as a first application of how tools from geometric mechanics can provide insight into the character and principles of legged locomotion.

## 1 Introduction

Many studies of terrestrial locomotion have focused on interaction with rigid, flat laboratory trackways. However, organisms often live on or within complex terrain that is flowable, loose, and wet (e.g. sand, dirt, or mud). In addition, organisms with different limb morphologies and kinematics likely evolved terrestrial locomotion strategies as they moved from oceans and lakes onto beaches of these flowable materials. When investigating principles of biological locomotion, it has proved useful to build robots with analogous capabilities. These robophysical models allow for tests of function and suggest hypotheses for mechanical and nervous system control.

To understand how vertebrates made the transition from water to land, we first analyzed the motion of mudskippers, modern analogs of early tetrapods, and showed that their tail is helpful for land locomotion, especially on sandy slopes [11]. Now we have begun to work on salamanders, another extant animal model for tetrapod evolution. Previous work focused on gait transition between swimming and walking by changing the frequency and amplitude of drive applied to the spinal cord of salamander robot [8]. As far as we know there has been little discussion on robustness and efficiency of tetrapod locomotion on deformable/flowable substrates. In this extended abstract, we aim to show experimentally and theoretically that coordinated body bending may improve the robustness of locomotion on challenging substrates. Recently, our group has developed a model using geometric mechanics (an area of research combining classical mechanics with differential geometry) to understand how shape changes relate to translations and rotations of the body during limbless locomotion on and in granular media [2, 6, 7, 11]. In this extended abstract, we summarize our application of the model to legged locomotion providing further evidence that geometric mechanics can be used as a general framework and language for locomotion.

## 2 Experimental Setups and Robot Platform

### 2.1 Animal Experiments

Fire salamanders (*Salamandra salamandra*) (about 40 g, 15–20 cm long) (see Fig. 1-D) were placed at the end of long, narrow trackway ( $\sim 10$  cm wide,  $\sim 50$  cm long) filled with a 3-cm-deep layer of  $\sim 0.2$  mm diameter glass particles, see Fig. 1-B. A dark space (which the animal prefers) was provided at the other end of the track to encourage the salamanders to move. Five trials were collected for each of ten salamanders on level ground. The order in which individuals were used in experiments was randomized and animals were given at least a two minutes to rest after each trial. Videos of each experiment were recorded by three synchronized GoPro cameras (see Fig. 1-B). We observed that in the sand, animals adopted a gait in which at least three legs were on the ground at all times (see step diagrams and average step frequencies with standard deviation that shows the portion of a stride during which each foot is on the ground during one cycle in Fig. 3-B).

### 2.2 Robot Experiments

Using a *robophysical* approach [1], we built a salamander robot and have tested its performance on granular media. This open-loop, servo-driven, 3D-printed robot (450 g,  $\sim 40$  cm long) has four limbs, an actuated trunk, and an active tail (Fig. 1-C, E). Each limb has two servo motors to control the vertical position and the step size of the limb. A joint in the middle of the body controls horizontal bending. The design and materials allow us to easily change morphological parameters of the body and legs.

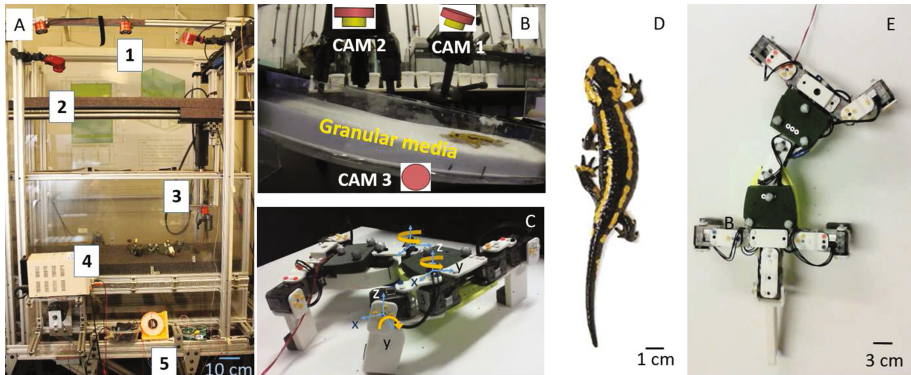


**Fig. 1.** Experimental setups, robophysical model and salamander. (A) The Systematic Creation of Arbitrary Terrain and Testing of Exploratory Robots (SCATTER) [12] system allows for automated three axis manipulation of robot traversing a granular substrate with specified surface incline. (1) Optitrack vision capture system (2) 3-axis stage (3) Gripper (4) Fluidized bed trackway filled with granular media (5) Tilting actuator (B) Animal experimental setup (C) Robot side view and servo angles (D) Top view of the fire salamander (E) Top view of the robophysical model

We performed experiments to systematically test the importance of body morphology, limb coordination, tail use and body flexibility on yielding substrates using a fully-automated setup [12], and compared the successes and failures of the robot with that of the animals. Our setup consists of four vacuums to prepare a uniform loosely packed state [10] in the trackway filled with  $\sim 1$  mm diameter poppy seeds before each experiment, tilting actuators to create inclined granular environments, a 3-axis motor system (Copley) to control the gripper position and four cameras (Naturalpoint, Flex13, 120 FPS) to capture the position and orientation of the robot (Fig. 1-A).

### 3 Geometric Mechanics Model

Geometric mechanics is a mathematical tool that relates internal shape changes (i.e. the joint angles) to net changes in translation and rotation of the body in world frame for a given interaction model with environment [9]. Previously, it was used to analyze a wide range of locomotor behaviors such as limbless locomotion [4]. Here we describe how it is also applicable to legged locomotion under several choices of modeling assumptions. Our legged-locomotor (Fig. 1-E) uses a lateral sequence, diagonal-couplet walking gait that is similar to animal salamander gait (three legs are on ground at each time step Fig. 2-A). The leg angle,  $\beta$ , is defined as the angle between the distal end of the limb and a line that is perpendicular to body transverse axis (see Fig. 2-B). We used a sinusoidally-varying leg angle (Fig. 2-D) and assumed that four legs followed the same gait but differed by phase,

$$\beta_i = \beta(t + \Delta\phi_i) \quad \text{and} \quad A_i(t) = A(t + \Delta\phi_i) \quad \text{for} \quad i = 1, 2, 3, 4, \quad (1)$$

where  $\beta$  and  $A$  describe leg angle and activation and are given by

$$\beta = \begin{cases} \sin\left(\frac{\pi}{2\tau_1}\tau\right) \\ \cos\left(\frac{\pi(\tau-\tau_1)}{\tau_2-\tau_1}\right) \\ -\cos\left(\frac{\pi(\tau-\tau_1)}{2(2\pi-\tau_2)}\right) \end{cases} \quad A = \begin{cases} \text{air} & \text{if } 0 < \tau < \tau_1 \\ \text{ground} & \text{if } \tau_1 < \tau < \tau_2 \\ \text{air} & \text{if } \tau_2 < \tau < 2\pi \end{cases} \quad (2)$$

To ensure the three legs are on the ground at the same time, the air phase of each leg must be coordinated in sequence. There are six combinations of leg phases that satisfy the tripod condition. Since the gait is periodic, we take FR as the first leg to move. The six combinations are listed in Fig. 3-A. We used the optimal body frame to represent the position and orientation of the robot, and the optimal frame is determined using the method described in [6]. This frame roughly sits at the average position of the two body links, and is aligned with the average orientation of the two body links. In the model, the position and orientation of the salamander head in world frame are defined as  $\mathbf{g} = [x, y, \theta]$ . We used shape space variables  $\mathbf{r} = [\alpha, \tau]$ , where  $\tau$  is leg phase and  $\alpha$  is body angle, to fully characterize the leg gait. For a mechanical system, the body velocity can be expressed by  $\mathbf{g}' = A(\mathbf{r})\dot{\mathbf{r}}$  where  $A(\mathbf{r})$  maps the shape variables to the body velocity.

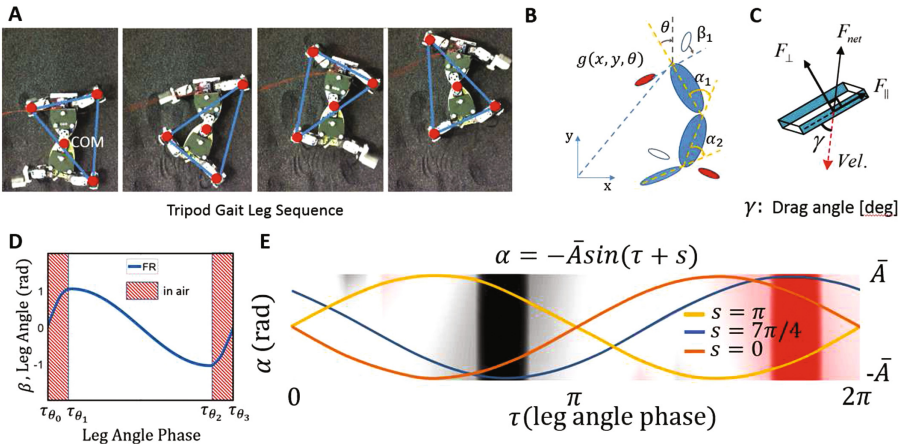


**Fig. 2.** Geometric mechanics applied to tetrapod locomotion on granular media. (A) Dorsal view of the sequence of support patterns during one stride of a lateral sequence, diagonal-couplet walk of robophysical model moving on granular media (B) Snapshot from the geometric mechanics model. The model has two body segments, a tail, and four limbs. The tail is inactive and always in contact with the ground. Leg colors define the activation, where red: legs are on ground and white: in air (C) The thrust and drag components of reaction force (Eq. 3) (D) An example nonlinear sinusoidal pattern of leg angle (E) Height function of the sinusoidal gait as a function of body angle  $\alpha$  and leg angle phase  $\tau$ . (Color figure online)

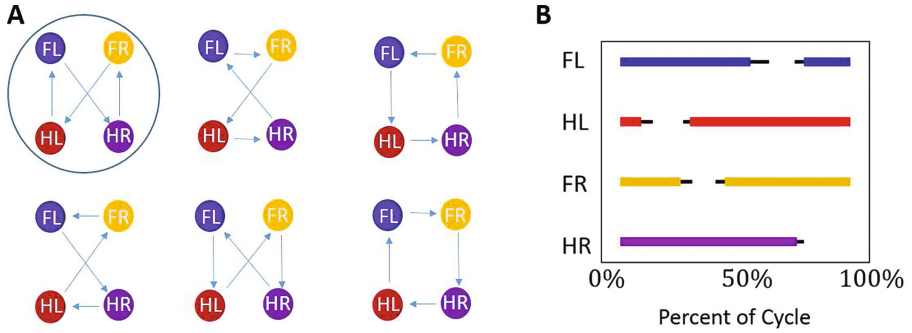


**Fig. 3.** Fire salamander's gait pattern. (A) Possible leg patterns of quadrupedal locomotion. In our studies the salamanders typically used the circled pattern. (B) Salamander step diagram H: hind, F: front, R: right, L: left, error bars indicated the standard deviations; data from three animals walking on level sandy ground, 13 steps in total, the average cycle duration is  $\sim 1.5$  s.

Granular resistive force theory (*RFT*) is used to model the movement of animals and robots in granular media [5, 11]. Prior work has shown simulations using granular *RFT* agreed well with actual robots [7, 11]. We therefore used granular *RFT* to numerically derive local connections. In granular *RFT*, the resistive force experienced on an infinitesimally small segment of a moving intruder is decomposed into thrust and drag components. The reaction force applied on the entire system is computed as,

$$\mathbf{F} = \int d\mathbf{F}_{\perp} + d\mathbf{F}_{\parallel} \quad (3)$$

where  $\mathbf{F}_{\perp}$  and  $\mathbf{F}_{\parallel}$  respectively denote forces perpendicular and parallel to a segment and are a function of attack angle,  $\gamma$  (Fig. 2-C) and are independent from the magnitude of speed [11]. The attack angle of a moving segment can be computed from its body velocity. We assumed the motion of the salamander-like robot in granular material is quasi-static, which means the total net force,  $\mathbf{F}$  applied on the system is zero. The only unknown in Eq. 3 is the velocity of the body frame. Given a shape velocity  $\mathbf{r}$  the body velocity of the average body frame can be computed numerically. To do that we uniformly sampled the two dimensional shape space on a grid where  $\tau \in (0, 2\pi)$  and  $\alpha \in (-\pi/6, \pi/6)$ . At every point  $(\alpha, \tau)$  on the grid, we first locally perturbed the value of first shape variable  $\alpha = \alpha + \epsilon$ , while holding the other constant. In practice, the magnitude of perturbation was  $\epsilon = 0.01$ . This small change in shape produces a small displacement  $[\Delta x_1^b, \Delta y_1^b, \Delta \theta_1^b]$ , measured in the body frame, which can be computed using the *RFT* calculation. Next, we kept the value of the first shape variable constant and perturbed second shape variable  $\tau = \tau + \epsilon$ . The resultant displacement and rotation measured in the body frame was  $[\Delta x_2^b, \Delta y_2^b, \Delta \theta_2^b]$ . These numerically calculated displacements served an approximation to the local connection at shape  $(\alpha, \tau)$ ,

$$J(\alpha, \tau) \approx \begin{bmatrix} \Delta x_1^b & \Delta x_2^b \\ \Delta y_1^b & \Delta y_2^b \\ \Delta \theta_1^b & \Delta \theta_2^b \end{bmatrix} / \epsilon \quad (4)$$

The same procedure was repeated at every sampled point. The displacement and rotation by a gait can be approximated by a line integral:

$$\begin{bmatrix} \Delta x \\ \Delta y \\ \Delta \theta \end{bmatrix} := \oint_{gait} J(\mathbf{r}) d\mathbf{r} \quad (5)$$

According to Stokes Theorem, the line integral along a closed gait is equal to the area integral of the curl of  $J(\mathbf{r})$  over the surface area enclosed by the gait:

$$\oint_{gait} J(\mathbf{r}) d\mathbf{r} = \iint_{gait} \nabla \times J(\mathbf{r}) d\alpha d\tau \quad (6)$$

The curl of connection vector field  $\nabla \times J(\mathbf{r})$  is referred to as the height function. Figure 2-E shows the height function of the sinusoidal gait used in this study. The largest displacement per cycle can be determined by finding the zero set which has the largest area integral. Therefore, the optimal body-leg coordination is obtained with the largest surface integral in the height function.

## 4 Results

In this section, we demonstrate how the parameterized gait model can be used to model salamander motion on level granular media. We first tested the six leg-lifting sequences (Fig. 3-A) according to a static stability criteria such that the CoM should remain inside the support polygon formed by the leg contacts at each time step. Theoretical leg sequences shown in bottom row of Fig. 3-A contain moments in which the CoM falls outside of the supporting polygon. We compared the other three sequences (given in top row of Fig. 3-A) and we see both experimentally and theoretically that FR-HL-FL-HR, which is also used by animals leads to a longer step length (Fig. 4-A). We took the FR-HL-FL-HR as a leg-lifting sequence and computed the step length (half of the distance between two successive placements of the same foot) experimentally and theoretically associated with the gait pattern. The height function introduced in Sect. 3 was calculated assuming that the body angle is sinusoidal, i.e.  $\alpha = -\bar{A} \sin(\tau + s)$  where  $\tau$  is the leg phase and  $s$  is the body phase-shift. According to theory, the optimal gait would enclose most surface integral in the height function (see Fig. 2-E). Apparently, the optimal body phase-shift would be  $7\pi/4$ , which encloses the most red and least black regions in the height function. To verify our theory, we tested eight different body phase-shifts given in Fig. 4-C both in simulation and experiment and the results indicate that the optimal body phase-shift is close the  $7\pi/4$ . In addition to varying the phase-shift, we varied amplitude of body bending,  $\alpha$  from 0 to  $50^\circ$ . We see also that body angle increases step length (see Fig. 4-B). The experimental results agree well with

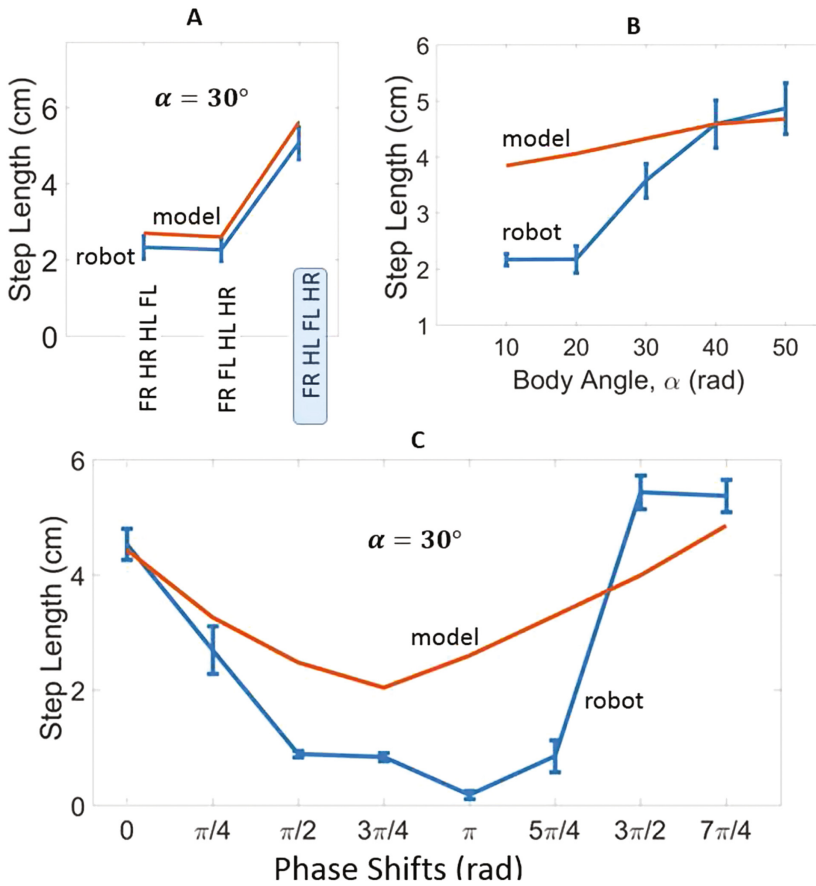


**Fig. 4.** Comparison of the model with robophysical experiments on level ground granular media. (A) Step lengths of the robot/model with four different leg sequences (FR: front right, FL: front left, HR: hind right, HL: hind left leg) (B) Step length vs. amplitude of body angle,  $\alpha$  (C) Step length changes as a function of phase shift between body and leg angles for  $\alpha = 30^\circ$ . Error bars denote standard deviation over 10 trials. (Color figure online)

the model for 40 and 50°. We posit that for the low amplitude region, the accumulation of the sand (especially on the posterior portion of the robot) decreases the step length, which is not considered in the model.

## 5 Conclusion

In this extended abstract, we summarized the application of techniques from geometric mechanics to model the locomotion of fire salamanders and a tetrapod robophysical model in a granular medium. Our study builds on our previous

successes in using geometric mechanics to model limbless locomotion in homogeneous environments [3,7], demonstrating that these tools can be applied to legged systems. We use the theory to compute an optimal gait in terms of leg-leg coordination (leg-lifting sequence) and body-leg coordination (body phase-shift) and compared our predictions with experimental data. We see that animals show a similar pattern to the optimal leg activation pattern predicted by theory. In the future, we will extend our study to understand behaviors like turning-in-place and to understand the role of appendage use on inclined sandy surfaces.

**Acknowledgment.** This work was supported by NSF Physics of Living Systems. We would like to thank Lucy Clarkson for her assistance with the collection of animal data, Christian Hubicki and the anonymous reviewers for their insightful comments/suggestions on the paper.

## References

1. Aguilar, J., Zhang, T., Qian, F., Kingsbury, M., McInroe, B., Mazouchova, N., Li, C., Maladen, R., Gong, C., Travers, M. and Hatton, R.L., Choset, H., Umbanhowar, P.B., Goldman, D.I.: A review on locomotion robophysics: the study of movement at the intersection of robotics, soft matter and dynamical systems. CoRR, abs/1602.04712 (2016)
2. Dai, J., Faraji, H., Gong, C., Hatton, R.L., Goldman, D.I., Choset, H.: Geometric swimming on a granular surface. In: Proceedings of Robotics: Science and Systems, AnnArbor, Michigan, June 2016
3. Gong, C., Goldman, D.I., Choset, H.: Simplifying gait design via shape basis optimization. In: Robotics: Science and Systems XII, University of Michigan, Ann Arbor, Michigan, USA, 18–22 June 2016
4. Gong, C., Travers, M.J., Astley, H.C., Li, L., Mendelson, J.R., Goldman, D.I., Choset, H.: Kinematic gait synthesis for snake robots. *Int. J. Robot. Res.* **35**(1–3), 100–113 (2016)
5. Gray, J., Hancock, G.J.: The propulsion of sea-urchin spermatozoa. *J. Exp. Biol.* **32**(4), 802–814 (1955)
6. Hatton, R.L., Choset, H.: Geometric motion planning: the local connection, stokes theorem, and the importance of coordinate choice. *Int. J. Robot. Res.* **30**(8), 988–1014 (2011)
7. Hatton, R.L., Ding, Y., Choset, H., Goldman, D.I.: Geometric visualization of self-propulsion in a complex medium. *Phys. Rev. Lett.* **110**, 078101 (2013)
8. Ijspeert, A.J., Crespi, A., Ryczko, D., Cabelguen, J.-M.: From swimming to walking with a salamander robot driven by a spinal cord model. *Science* **315**(5817), 1416–1420 (2007)
9. Kelly, S.D., Murray, R.M.: Geometric phases and robotic locomotion. *J. Robot. Syst.* **12**(6), 417–431 (1995)
10. Li, C., Umbanhowar, P.B., Komsuoglu, H., Koditschek, D.E., Goldman, D.I.: Sensitive dependence of the motion of a legged robot on granular media. *Proc. Natl. Acad. Sci.* **106**(9), 3029–3034 (2009)

11. McInroe, B., Astley, H.C., Gong, C., Kawano, S.M., Schiebel, P.E., Rieser, J.M., Choset, H., Blob, R.W., Goldman, D.I.: Tail use improves performance on soft substrates in models of early vertebrate land locomotors. *Science* **353**(6295), 154–158 (2016)
12. Qian, F., Zhang, T., Daffon, K., Goldman, D.I.: An automated system for systematic testing of locomotion on heterogeneous granular media. In: *International Conference on Climbing and Walking Robots (CLAWAR)* (2013)